Hindawi
Mobile Information Systems
Volume 2022, Article ID 6168361, 10 pages
https://doi.org/10.1155/2022/6168361

Research Article

Design of Multipoint Temperature and Humidity Silverware Forging for Engraving Process Measurement System Based on ZigBee Technology

Jinye Wei[1,2] **and Jiaqian Leng**[1,2]

[1]*King Mongkut's Institute of Technology Ladkrabang, Ladkrabang District, Bangkok 10520, Thailand*
[2]*Nanning University, Nanning, Guangxi 530200, China*

Correspondence should be addressed to Jiaqian Leng; lengjiaqian@nnxy.edu.cn

Received 12 June 2022; Accepted 20 July 2022; Published 13 August 2022

Academic Editor: Shadi Aljawarneh

This paper studies an embedded monitoring system centered on ZigBee technology to realize real-time temperature and humidity monitoring, and to ensure low power consumption, high reliability, low cost, and collection of environmental information. The communication is designed using the star topology, and the whole network structure is composed of a master node and three sensor receiving nodes to realize the unlimited transmission of network data. The main control point is to determine the coordination of the scope of the ZigBee network configuration system. The ZigBee network can communicate with the host through the data port to realize the acceptance of temperature and humidity data and the sending of commands. Based on this research, this paper determines the impact of non-target parameters on the actual measurement data of the multipoint temperature and humidity sensor, and at the same time determines the key influencing factors. For HMP-45D multipoint temperature and humidity, an improved genetic algorithm (GA) combined with a support vector machine (SVM) is used to compensate humidity and temperature data, which is designed to affect the actual measurement error of the multipoint temperature and humidity sensor. This paper studies the silver forging process, compares the environmental factors of silver carving, further puts forward the control strategy of Hagoun product forging and carving environment control from the perspective of temperature and humidity, and designs the environmental temperature and humidity measurement and control system from the perspective of temperature and humidity control. The system design proposed in this paper is mainly to construct and apply the silverware forging and engraving environment temperature and humidity measurement and control system on the basis of integration and maintenance-free and verify the effectiveness and feasibility of the system in the protection of cultural relics.

1. Introduction

ZigBee technology is widely understood as an energy-efficient network operation and a large-scale wireless communication protocol. We can also use routing methods to establish a theoretically unlimited communication network. ZigBee network technology is more complex and powerful than infrared, Bluetooth, and other network structures. ZigBee is widely used in various production and life fields, such as industrial production, environmental monitoring, commercial automation management, and automotive automation production. The world's leading manufacturers generally pay attention to the development of ZigBee technology and have great confidence in the future of the ZigBee market. At the same time, the ZigBee Technology Alliance is also expanding, cooperating with a number of chip manufacturers and software developers to establish a standardized organization. ZigBee technology is expected to have broader development prospects worldwide.

In this article, we designed a multipoint temperature and humidity measurement terminal, which is the core unit, uses ZigBee technology to implement unlimited communication, and collects multi-channel sensor data from the base station wireless network. The wireless base station control center is

equipped with an AT91SAM9263 microprocessor and combined with CC2530. This is a chip-based system that supports ZigBee applications and large SD card memory devices for multi-processor operation. The measurement result is controlled by the low power consumption of MSP430F2618. The core downloads the multifunctional humidity measurement dimension through the CC2530 wireless network module with field measurement, network connection, stability temperature sensor, and HHC2-S humidity sensor. This article introduces a network application program that supports multitasking with the Layer operating system, and the research and development of the ZigBee network based on the Z protocol stack of FA Enterprise.

Finally, through the detailed study of the silver forging process, this paper further expounds its processing technology and characteristics, analyzes the development status of the silver forging process and its application in modern metal technology, and applies ZigBee technology to silver forging and carving environment. The precise control and environmental humidity of the system are designed, and the hardware and software designs of the entire system are introduced in detail. It can be seen that +0.3°C means that the system temperature measurement accuracy can reach the level, and ±1.5% means the humidity measurement accuracy can reach the level. The humidity control accuracy can reach 3%. In addition, the maintenance-free automatic water replenishment function facilitates the temperature and humidity environment of silverware forging and engraving its own products. After experimental testing and field application, the system runs stably and reliably, and the measurement accuracy meets the design requirements.

2. Related Work

The literature introduces the traditional Gumgang handicrafts and modern hand-painted forgings applied to the craftsmanship and technology restoration and retains the craftsmanship and artistic characteristics of sculptures in some ethnic minority areas in southwest China. As a process of accumulation of cultural origin and experience of hand forging, it supports and promotes the development of hand forging technology. The literature introduces a wireless temperature and humidity monitoring system based on ZigBee technology, which allows temperature and humidity sensor modules to monitor temperature and humidity in real time within the network of the monitoring center; some literature describes the hardware design of the system [1, 2]. First, this paper introduced the technical advantages of ZigBee wireless sensors in the network. Based on the advantages of ZigBee, we will explain in detail the overall design of the farm's wireless temperature and humidity monitoring system, including the basic hardware configuration, software flow, and hardware based on ZigBee radio temperature and humidity monitoring [3]. And we create software according to the hardware structure, apply it to the temperature and humidity monitoring of the breeding field, realize the temperature and humidity monitoring of the breeding field, and analyze the experimental results. The literature introduces the star topology network structure and creates a method to improve the accuracy and reliability of the equipment in the software and hardware [4]. Experiments show that the key indicators of the equipment have reached the level of domestic and foreign products [5]. The literature introduces the main design of the single-chip microcomputer, using multiple sensors to collect data of temperature and humidity parameters under the control of the single-chip microcomputer. The system is mainly composed of temperature measurement theory, analog circuit, digital circuit, digital filtering algorithm, and single-chip microcomputer [6].

3. Model Design of Multipoint Temperature Based on ZigBee Technology

3.1. ZigBee Technology and Protocol. With the rapid development of semiconductor technology and communication technology in the world today, new short-range wireless communication devices have appeared one after another, and gradually replaced wired devices, occupying most of the market share [7]. In the 21st century, various non-technologies have been quite mature. Mid-infrared technologies such as Bluetooth technology and radio frequency technology have been widely used in production and life.

This technology is a new type of wireless touch network, which is becoming more and more common in low-speed wireless networks. It mainly utilizes the advantages of short distance, low data rate, low power consumption, and low cost, and is used for intelligent control and short distance wireless communication, and can be integrated into general equipment to develop a small and economical wireless sensor network [8]. The traditional ZigBee protocol structure is uniformly regulated by the ZigBee Technology Alliance. Figure 1 shows a block diagram of each layer structure.

The functions of data transmission and management tasks in the higher layer of the ZigBee protocol are provided and supported by the lower layer. After years of innovation and years of user practice by the ZigBee Alliance, the topology of the ZigBee network changes every day. Today, the most widely used network topologies in the world include star, mesh, and tree structures.

(1) Type topology: The star topology is the core of the entire network and is generally located in the center of the network. It can establish and maintain the star network in real time. The RFD node is responsible for implementing specific development functions [9]. This device can not only receive the signals obtained from the sensors, but also directly communicate with the coordinator. It is the connection channel between the outside world and the central controller. Of course, the coordinator can also be used on the terminal device, and all data must pass through the coordinator.

The star topology is structurally flexible and has poor portability. Each node must be connected to the coordinator, reducing the overall structure of the

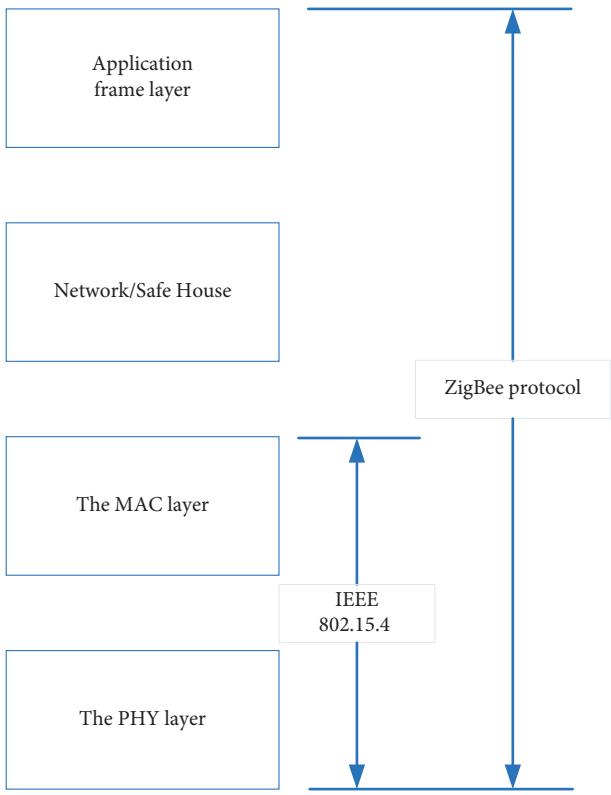

Figure 1: ZigBee protocol structure.

network [10]. Many endpoint devices are susceptible to network data expectations and other phenomena, leading to serious data loss. Due to structural commonality, if the ZigBee coordinator is abnormal, the entire network cannot continue to operate.

(2) Mesh topology: In contrast, the mesh topology is safer and more reliable. The entire network is usually coordinated by multiple coordinators to form the framework of the network. They are the same as each other and can transmit data between each node and the coordinator within the range. Each RFD can be used to tune the entire system, but it can only be tuned once [11]. The ownership of the coordinator is regulated by the upper network. Once the coordinator is confirmed, it can manage the functions of the entire network and bind the connection of each device without simply sending other data.

The mesh topology provides highly reliable performance and can be automatically created, organized, and self-repaired, so that it can quickly adapt in harsh environments. The path of data transmission is selectable in the network structure, rather than a single one, thus avoiding the possibility of network paralysis [12]. The variable coordinator will increase the time in the data transmission process, and at the same time will increase the network complexity and power consumption.

(3) Tree topology: A group of tree structures can be formed by connecting multiple groups of star combinations. Like the grid structure, the tree nodes are all composed of FFD, and the ownership of the coordinator is determined by the upper network. The end nodes of the network usually use RFD for operation and will also provide FFD under any circumstances [13].

3.2. Multipoint Temperature and Humidity Measurement Technology. The HMP-45D Pt100 Platinum resistance temperature sensor is manufactured by photolithography technology. The metal has high purity, good stability, and good reproducibility, is very sensitive to changes in ambient temperature, and has accurate reproducibility. Its value is 10^{-4}. Because of these characteristics, platinum resistors are often used to create laboratory standard equipment for instrument measurement and calibration [14]. The platinum resistance temperature measurement is based on the linear relationship between the platinum resistance conversion amount and the ambient temperature value. The relationship between resistance value and temperature value is reflected in formulas (1) and (2).

$$R_t = R_0 + \left[1 + At + Bt^2 + C(t-100)t^3\right] \quad -50 < t < 0^{\circ}C, \tag{1}$$

$$R_t = R_0 * \left[1 + At + Bt^2\right] \quad 0 < t < 80^{\circ}C. \tag{2}$$

The most important parameters of a moderately sensitive capacitive sensor are the capacitance value and quality factor. Among them, the production level is directly determined by the quality of the capacitor. The capacitance value C is obtained by measuring the circuit. In fact, the capacitance change is very small (usually less than 50pF), so the small capacitance value is converted to a voltage value between 0 V and 1 V by a high-frequency conversion circuit. The relationship between the last measured capacitance value and humidity value is corrected.

The corresponding relationship between the capacitance value of the humidity-sensitive capacitor and the relative humidity is described in formula (3).

$$C = \varepsilon_0 \varepsilon_r \frac{S}{D}. \tag{3}$$

Through the analysis of formula (3), it can be known that the dielectric constant, the effective relative area of the electrode plate, and the film thickness directly determine the capacitance value of the humidity-sensitive capacitor. Similarly, according to the characteristics of the material, temperature changes have little effect on the effective mating area of the storage substrate but have a greater effect on the humidity-sensitive film thickness [15, 16]. As the ambient temperature increases, heat will cause the humidity-sensitive film to expand and reduce its capacitance value, but there is a positive correlation between the effective area S and the capacitance value C [17]. In other words, the capacitors that are sensitive to humidity due to temperature changes have different effects, and the inevitable mathematical connection between the two cannot be expressed in the functional relationship [18, 19].

The humidity sensor is susceptible to interference from the ambient temperature when measuring relative humidity, and the actual humidity data observed will be displayed in a nonlinear manner. To correct the temperature nonlinear error interference in the observed data value of the humidity sensor, the mathematical model of the humidity sensor is:

$$y = f(x,t). \tag{4}$$

The inverse function of formula (5) is:

$$x = f^{-1}(y,t). \tag{5}$$

Formula (5) shows that relative humidity and ambient temperature are used as model input data to finally eliminate the measurement error caused by temperature t.

Start with limited sample data to obtain the best generalization ability to find the best balance between the complexity of the SVM algorithm and the learning ability. Compared with the empirical risk minimization model, the support vector machine can effectively prevent the local extreme and the "over-learning" state from showing certain advantages [20–22].

At the same time, in order to improve the fault tolerance of the support vector machine regression algorithm model, the relaxation factor F_i, ξ_i^* and the penalty factor C are introduced to perform the nonlinear conversion. Equation (6) provides an optimal solution to the problem:

$$\left\{\frac{1}{2}\|w\|^2 + C\sum_{i=1}^{l}(\xi_i + \xi_i^*)\right\},$$

$$\text{s.t.} \quad \left\{\begin{array}{l} [(w\cdot x_i + b)] - y_i \le \varepsilon + \xi_i \\ y_i - [(w\cdot x_i + b)] \le \varepsilon + \xi_i^* \\ \xi_i, \xi_i^* \ge 0, \quad i = 1,2,\cdots,l \end{array}\right\}. \tag{6}$$

Use the Lagrange multiplier to transform it into a dual problem:

$$\max\left\{\sum_{i=1}^{l}\alpha_i - \frac{1}{2}\sum_{i=1}^{l}\sum_{j=1}^{l}\alpha_i\alpha_j y_i y_j K(x_i, y_j)\right\},$$

$$\text{s.t.} \quad 0 \le \alpha_i \le C, \frac{1}{2}\sum_{i=1}^{l}\alpha_i y_i = 0. \tag{7}$$

Solving (7), we get:

$$w = \sum_{i=1}^{l}\alpha_i y_i x_i,$$

$$b = y_i - \sum_{i=1}^{l} y_i\alpha_i(x_i \cdot x_j). \tag{8}$$

Finally, the discriminant function is obtained:

$$f(x) = \operatorname{sgn}\left(\sum_{i=1}^{l}\alpha_i y_i K(x\cdot x_i) + b\right). \tag{9}$$

It can be seen from the above that SVM processes the data in the original sample space and uses the kernel to map it to a higher-dimensional space. The establishment of the classification plane can effectively avoid the disaster of dimensionality. Use the RBF kernel function that obeys the Gaussian distribution, that is

$$K(x_i, y_j) = \exp\left(\frac{-\|x_i - x_j\|^2}{(2*\alpha^2)}\right). \tag{10}$$

When establishing the SVM algorithm compensation model, it is necessary to accurately select the SVM algorithm parameters, but nowadays, the parameters are mainly selected through empirical methods, grid parameter optimization methods, etc. These parameters cannot guarantee the performance of further optimization. The SVM algorithm compensation model requires in-depth research on the solution of selecting SVM parameters.

In the process of genetic algorithm, the genetic information of each parent tends to be the same, which slows down the speed of genetic evolution or even interrupts the evolution, so that the genetic evolution reaches the local optimal solution. Therefore, it is necessary to select the best fitness function, optimize the genetic operator and parameter optimization, and improve the selection of genetic selection, crossover operator, adaptive crossover probability pc, and mutation probability pm. The specific improvements are as follows

The fitness function explains the prediction accuracy of the SVM algorithm and determines the direction of the algorithm's development. The specific situation is shown in formula (11):

$$MSE = \frac{1}{l}\sum_{i=1}^{l}(y_o - y_i)^2. \tag{11}$$

The objective function is:

$$\text{fitness}(i) = \frac{1}{MSE}. \tag{12}$$

The first is to optimize the genetic operator. At the same time, the operation of the operator is relatively simple, which can better ensure the diversity of population information, so it has been widely used. However, due to the random selection function, the algorithm has selection errors or unnecessary deterioration. Therefore, this article introduces the elite storage system and the classified working set into the traditional roulette selection algorithm. First, calculate the physical fitness values of all individuals, classify them from small to large according to their sizes, and then select and save the best individuals with the largest physical fitness values from the previous generation of 5%×n population; perform for the remaining individual's Roulette selection, ensuring individual safety (95% × n − 1), crossover and

mutation, to ensure the safety of all individuals in the next generation.

In addition to improving and optimizing genetic operators, it is also necessary to adjust the crossover probability and mutation probability according to the similarity of the parental genetic information. If the personal differences between parents are large, a larger probability of crossover and a smaller probability of change are needed to store good parental information. If the personalized information tends to be consistent, a smaller crossover probability and a higher mutation probability are required to maintain the diversity of demographic information and avoid falling into the regional optimal solution. Based on the individual similarity, crossover, and change probability, when $r > r_0$ is adjusted, as shown in formulas (13) and (14).

$$p_c = \begin{cases} p_{c1} * \left[\dfrac{r - r_0}{r} + \dfrac{f_{\max} - f}{f_{\max} - f_{\text{avg}}} \right], & f_{\text{ong}} \le f, \\ p_{c2} * \dfrac{(r - r_0)}{r}, & f_{\text{ang}} > f, \end{cases} \tag{13}$$

$$p_m = \left\{ p_{ml} * \left[\frac{r - r_0}{r} + \frac{f_{\max} - f'}{f_{\max} - f_{\partial v_o}} \right], f_{mg} \le f'. \right. \tag{14}$$

3.3. System Energy Consumption Control. The wireless measurement terminal designed in this paper adopts a specific energy consumption control strategy, which can make the system reduce power consumption. In order to ensure the stable operation of the system, reducing the use of auxiliary power is the basic method to solve the problem of system energy consumption. From the perspective of theoretical analysis, this article discusses how the system effectively uses battery power, balances the overall energy consumption of the control network, and maximizes the system's stable running time.

Based on the modular design of the wireless measurement terminal, the main part of the additional energy consumption in the wireless measurement terminal is the microprocessor module as the wireless communication module and the user interface module. The current running statistics of each module is shown in Figure 2.

Modules with high energy consumption are the main goal of controlling energy consumption. For liquid crystal displays, the steps taken are relatively simple, and program control can save money and make the most of them. After the mechanical interface stops working, by turning off the LCD power supply, the energy consumption of personnel can be reduced. When an operation on the mechanical interface is triggered, a new man-machine interface will be displayed on the LCD display. In order to realize the network communication of the system, energy consumption must be controlled under the premise of ensuring the quality of network communication. We will study and analyze the power consumption of wireless ZigBee networks.

This article uses a simple model to illustrate the energy consumption of wireless communication processing. Wireless communication includes wireless transmission and wireless reception. Transmission energy consumption includes transmitter energy consumption and drives circuit energy consumption. The transmission distance is the energy loss of the wireless communication module to transmit data between the next two nodes:

$$\begin{aligned} E_{Tx}(k,d) &= E_{Tx-\text{elec}}(k) + E_{Tx-\text{amp}}(k,d) \\ &= \begin{cases} kE_{\text{elec}} + k\varepsilon_{\text{friss-amp}} d^2 & d < d_{\text{crossover}}, \\ kE_{\text{elec}} + k\varepsilon_{\text{two-ray-amp}} d^4 & d > d_{\text{crossover}}, \end{cases} \\ E_{Rx}(k,d) &= E_{Rx-\text{elec}}(k) = kE_{\text{elec}}. \end{aligned} \tag{15}$$

Generally, the power consumption of the circuit is considered to be the same during transmission and reception. Because the energy consumption coefficients of the radio frequency amplifier are $\mathscr{E}_{\text{friss-amp}}$ and $\mathscr{E}_{\text{two-ray-amp}}$ respectively. Then, the coefficients of the model are:

$$\begin{aligned} E_{\text{elec}} &= \frac{50nJ}{\text{bit}}, \\ \varepsilon_{\text{friss-amp}} &= \frac{10pJ}{\text{bit}/m^2}, \\ \varepsilon_{\text{two-ray-amp}} &= \frac{0.0013pJ}{\text{bit}/m^4}. \end{aligned} \tag{16}$$

Because the main source of consumption is the transmission and reception of data. Therefore, active energy consumption control is performed during data transmission. Through wireless, reducing power and reducing energy consumption is the most direct and effective control method.

Assuming that the distance between nodes on the communication link of the router is the same as that of the coordinator, and k-bit data is sent to the coordinator at a fixed time interval, the node n farthest from the coordinator is forwarded to the node $n-1$ The energy consumption is as follows:

$$E_n = kE_{\text{elec}} + k\varepsilon d^2. \tag{17}$$

In addition to sending k-bit data from node $n-1$ to node $n-2$, it is also necessary to forward the k-bit data of node n. The energy consumption of node $n-1$ is as follows:

$$E_{n-1} = 3kE_{elec} + 2k\varepsilon d^2. \tag{18}$$

The energy consumption of the nth node and the mth node in the communication link can be estimated:

$$\begin{aligned} E_m &= (2n - 2m + 1)kE_{\text{elec}} + (n - m + 1)k\varepsilon d^2, \\ E_1 &= (2n - 1)kE_{\text{elec}} + nk\varepsilon d^2. \end{aligned} \tag{19}$$

By comparison, we can see that the energy consumption of the nth node is less than the energy consumption of the first node, and as the depth gradually increases, the difference is more obvious.

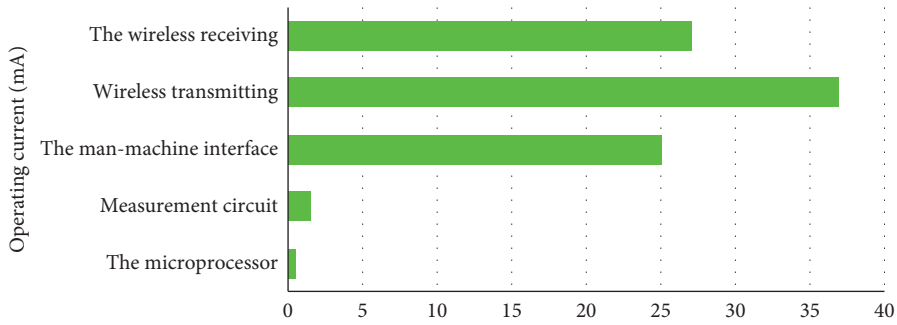

Figure 2: Energy consumption of each module of the wireless measurement terminal.

Based on the questions in the previous section, researchers have proposed various measures and methods to improve the life cycle of the network without supplementing energy. This section analyzes, compares, and proposes solutions to control the energy consumption of a single node and the difference in energy consumption between network nodes, and how to optimize energy consumption control strategies. The node residual energy model can be embodied in formula (20):

$$\begin{aligned} E_{\text{left}} &= E_0 - E_{Tx} - E_{Rx} \\ &= E_0 - \left(E_{\text{elec}} + \varepsilon_{\text{friss-amp}} d^2 E_{\text{elec}} + \varepsilon_{\text{friss-amp}} d^2\right) k_T - E_{\text{elec}} k_R. \end{aligned} \tag{20}$$

Considering the application of the system, during the measurement process, the nodes will not move their positions after placement, and in most cases, each node will transmit data to the coordinator along a fixed routing path. Each node transmits data at a fixed sampling interval, then:

$$\begin{aligned} k_T &= n_T \cdot t, \\ k_R &= n_R \cdot t. \end{aligned} \tag{21}$$

Equation (20) is further changed to

$$E_{\text{left}} = E_0 - \left(E_{\text{elec}} + \varepsilon_{\text{friss-amp}} d^2\right) \cdot n_T \cdot t - E_{\text{elec}} \cdot n_R \cdot t. \tag{22}$$

3.4. Energy Consumption Simulation. The simulation result is shown in Figure 3. In the left figure, we can see the simulation results that do not control the energy consumption, the nodes close to the coordination transfer a large amount of data, and the energy consumption is very fast, becoming the first dead node. The picture on the right uses a control strategy based on dynamic coordination. Due to node load distribution, most nodes will consume energy and leave the network until the first dead node appears in about 45,000 seconds. In a relatively short period of time, if the number of remaining nodes is the total number of nodes, the simulation time used by the two methods is similar. The last remaining node is the eccentric end node, because it does not need to transmit data from other nodes and consumes the least energy.

The node residual energy analysis calculates the residual energy of all nodes when the network is disconnected. The simulation result is shown in Figure 4. The left picture does not use the energy balance method, so when the first node is displayed, the remaining nodes have more energy and the energy distribution range is larger. The right figure uses a dynamic coordinated control strategy. From the results in the figure, the dynamic adjustment strategy has achieved a better energy balance effect.

Through the above simulation analysis, we can see that the area around the coordinator node in the wireless ZigBee network is the area with the highest energy consumption in the entire network. Nodes in this area need to transmit data from remote nodes. Therefore, it consumes the fastest energy. The main function of energy optimization control is to coordinate multipath from energy-intensive domain data to reduce the excessive energy consumption of certain nodes and balance the energy load of the entire network, thereby improving energy efficiency. The simulation results show that the energy optimization control has a positive influence on the nodes in the energy-intensive area.

4. Practical Application of Multipoint Temperature and Engraving Process

4.1. Overall Design of Multipoint Temperature and Humidity Measurement System. The system is mainly used for temperature and humidity measurement and control research. The system uses Palm certified Codewarrior 5.0 development platform. Compared with assembly language, C language has readability, flexibility, efficiency, module design and development, and rich library functions. This system is suitable for project management and multiple management.

System software design mainly includes the following parts: design temperature and humidity acquisition program, design humidity control program, design system communication software, and design human–computer interaction. The whole system of the system software is shown in Figure 5.

4.2. System Data Collection and Communication. Table 1 lists the communication protocol between the single-chip computer and the sensor module.

Serial communication is the basic method for the microprocessor to exchange data with the outside world. Few transmission lines are used for communication connection lines, and binary data sets are transmitted in bit order to share time in the software. MC9S12XS128 has two full-

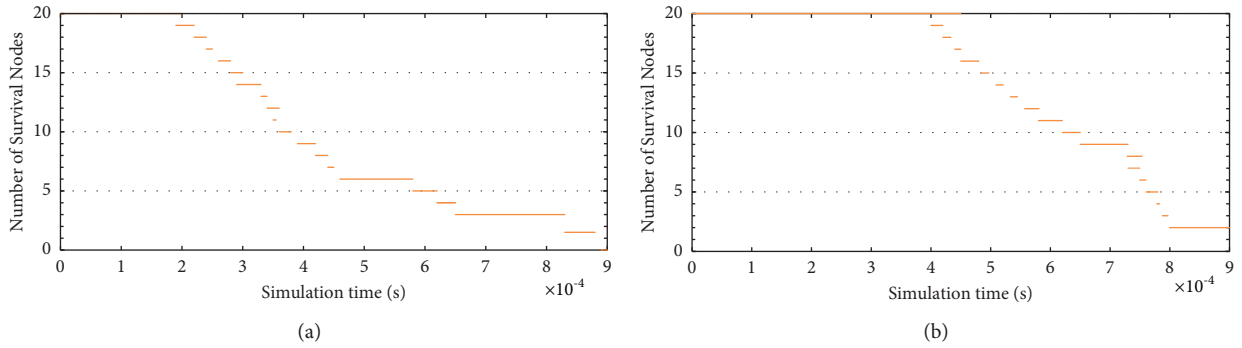

Figure 3: Network life cycle simulation without energy consumption control (a) and dynamic adjustment energy consumption control (b).

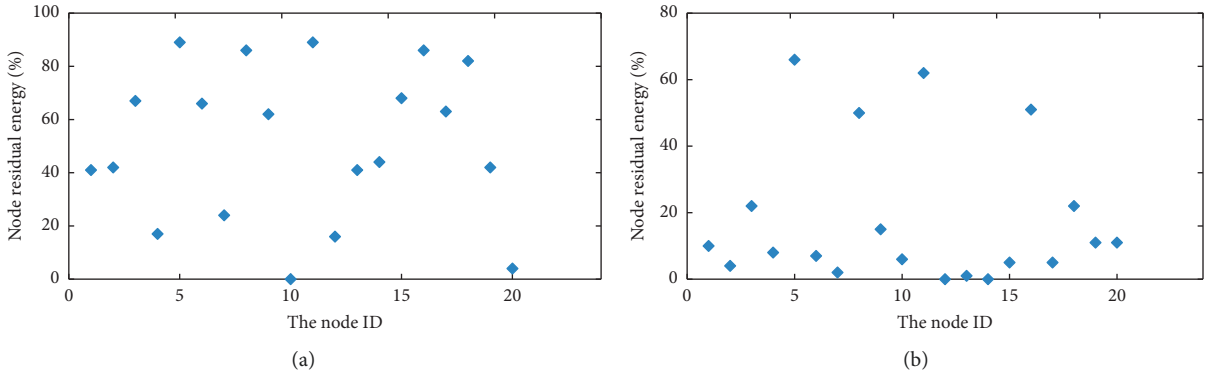

Figure 4: Node residual energy simulation without energy consumption control (a) and dynamic adjustment energy consumption control (b).

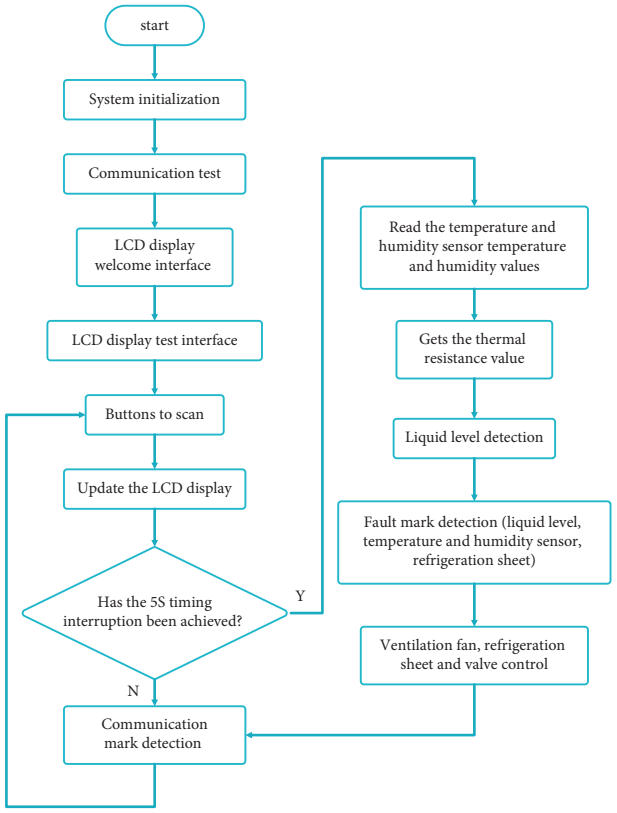

Figure 5: Overall block diagram of system software.

duplex serial communication interfaces SCI. The design uses query mode to enable data transmission and interrupt mode to enable data reception.

In order to ensure the integrity and reliability of the communication information, a more stringent communication protocol has been set up for data analysis communication. The specific content is shown in Table 2.

The communication protocol format is shown in Table 3.

In the second agreement, the sequence of data content is shown in Table 4.

In Article 4 of the agreement, the sequence of data content is shown in Table 5.

All numerical data are represented by high and low bytes.

In the 5th agreement, the data sequence of the temperature and humidity parameters to be set is shown in Table 6.

4.3. System Interface Design. After powering on the system, the "Welcome" interface will be displayed. After about 1 second, it will enter the inspection interface of the system itself to display the operating status of the device, the humidity setting target value, and the upper and lower limits of humidity. After 2S, go to the main data display interface, which displays the latest temperature and humidity data and the current time.

Table 1: Communication protocol between temperature and humidity monitor and sensor.

Serial number	Content	Number of bytes	Data flow direction	Remarks
1	52 18 3F 0A	4	Controller-sensor	Get temperature
2	48 16 temperature value corresponds to ASCII code 0A	7	Controller-sensor	Send temperature
3	52 20 3F 0A	4	Controller-sensor	Get humidity
4	48 16 humidity value corresponds to ASCII code 0A	7	Controller-sensor	Send humidity

Table 2: Communication protocol between temperature and humidity monitoring system and data analyzer.

Serial number	Character (data packet)	Content	Direction
1	A (0x41) + instrument address (0x01) + D (0x44) + instruction length (0x03) + data reserved byte (OxAA OxBB) + CRC (IB) 7 bytes in total	Intelligent data analysis loads temperature and humidity sensors and device status data into temperature and humidity monitors	Intelligent data analyzer-temperature and humidity monitor
2	a (0x61) + instrument address (0x01) + d (0x64) + instruction length (OxOB) + data content (10B) + CRC (1B) total 15 bytes	The temperature and humidity monitor sends temperature and humidity sensors and device status data to intelligent data analysis	Temperature and humidity monitor an intelligent data analyzer
3	A (0x41) + instrument address (0x01) + G (0x47) + instruction length (0x03) + data reserved byte (OxCC OxDD) + CRC (IB) 7 bytes in total	Intelligent data analysis can read the current temperature and humidity settings on the temperature and humidity monitor	Intelligent data analyzer-temperature and humidity monitor
4	a(0x61) + instrument address (0x01) + g (0x67) + instruction length (0x24) + data content (35B) + CRC (1B) 40 bytes in total	The temperature and humidity monitor feeds back the current temperature and humidity settings to intelligent data analysis	Temperature and humidity monitor-intelligent data analyzer
5	A (0x41) + instrument address (0x01) + S (0x53) + instruction length (OxOF) + temperature and humidity parameters to be set (14B) + CRC (IB) 19 bytes	Intelligent data analysis sends the set temperature and humidity parameters to the intelligent temperature and humidity monitor	Intelligent data analyzer-intelligent temperature and humidity monitor
6	a (0x61) + instrument address (0x01) + s (0x73) + instruction length (0x03) + data content (2B) + CRC (1B) 7 bytes in total	The intelligent temperature and humidity monitor can respond to the intelligent data analysis of the successfully set temperature and humidity parameters	Intelligent temperature and humidity monitor intelligent data analyzer

Table 3: Basic format of communication protocol.

Packet header (byte)	Instrument address (byte)	Function type (byte)	Data length (byte)	Data content	Check digit (byte)
1	1	1	1	*N* bytes	1

Table 4: Protocol 2 data content sequence.

Serial number	1	2	3	4	5
Name	Temperature value	Humidity value	Operation/fault	Humidification/dehumidification	Reserved byte
Number of bytes	2	2	1	1	4

Table 5: Protocol 4 data content sequence.

Serial number	1	2	3	4
Name	Humidity target value	Upper limit of humidity	Lower limit of humidity	Reserved byte
Number of bytes	2	2	2	8

Table 6: Protocol 5 data content sequence.

Serial number	1	2	3	4
Name	Humidity target value	Upper limit of humidity	Lower limit of humidity	Reserved byte
Number of bytes	2	2	2	8

Table 7: Button name and function description table.

Name	Function description
SET	(1) On the monitoring interface, press this key to enter the function setting (2) It is used to jump to the next configuration item in the configuration interface of the function
OK	Return to the status display interface in the function configuration interface, and complete the confirmation for confirming certain selections
LEFT	(1) Function configuration interface 1 is used to adjust the position of the selected item (2) The function configuration interface 2 is used to move the position of the selected number to the left
RIGNT	(1) Function configuration interface 1 is used to adjust the position of the selected item (2) The function configuration interface 2 is used to move the position of the selected number to the right
UP	The function configuration is used to increase the value of a specific number in interface 2
DOWN	The function configuration is used to increase the value of a specific number in interface 2

When the setting key is pressed from the main LCD display interface, it enters the setting state, initializes the setting data, and then determines the value of the next key. When entering this interface for the first time, the cursor will highlight the first position of the configuration, otherwise the cursor will remain at the last position when exiting the configuration interface last time. The left and right keys are used to change the cursor position, the up and down keys are used to increase or decrease the number, the set key is used to decrease the position bar, and the enter key is used to set the current value. The OK key is used to save the current values, exit the status and position setting interface, and return to the main display interface. Button name and function description are shown in Table 7.

4.4. Status Quo of Silver Forging and Engraving Process. China's Miao, Bai, Tibetan, and other ethnic minorities still use forging and carving techniques. This minority still maintains traditional handicrafts such as hammering and engraving ,and maintains certain traditional lifestyles and customs of its national culture. Due to the difference in development, we mainly study the hammering and engraving techniques of the Bai and Tibetans.

In addition to preserving and retaining the hammering and engraving techniques of some ethnic minorities, modern folk literature and art are also used for the restoration of handmade jewelry artifacts. The restoration of cultural relics is a very important task of the Archaeological Museum. The metal restoration techniques in the restoration of cultural relics include gold restoration, bronze restoration, and tin restoration. The original production process of cultural relics is mainly used after restoration to ensure the unity and integrity of cultural relics. It is a targeted crafting technique. For traditional Gumgwaung restoration techniques, hammering and engraving techniques are used in museums and archaeological projects. The restoration of cultural relics is diverse, complex, and targeted. Therefore, the restoration of cultural relics usually requires the comprehensive use of several technical tools. Cultural relic restoration workers inherit the traditional hammering and engraving techniques so that traditional techniques can reproduce the historical truth.

The theme of the development of modern metal craftsmen is to discuss the inheritance of traditional handicrafts and reflect the spirit of the times under contemporary art concepts. Hand forging includes the tradition and history of forging and engraving technology. The origin and development of forging and engraving technology continue to absorb production experience and use manual methods to express the author's creative ideas in the context of the new era. With the development of productivity, technology is constantly updated and improved. It is based on the experience of the predecessors and continues to innovate on this basis. As a new kind of handicraft, hand forging by modern metal craftsmen has special aesthetic importance. Traditional metal crafts often emphasize the beauty of the material itself and the value of the material, especially the artificial products with the greatest function made of the material. As a new kind of artwork, handicrafts may be eliminated, abandon the concept of utilitarianism, focus on pure artistic expression, and have a clearer aesthetic tendency. In the process of constantly seeking modern design, we are committed to expanding the expressive power and charm of metal materials, transcending the functional scope of materials, and giving them more spiritual and cultural meanings.

5. Conclusion

Since the advent of ZigBee wireless communication technology, it has been receiving extensive attention for its unique features such as simple protocol, low cost, powerful functions, and strong interference capabilities. At the same time, we will gradually expand to other areas, such as automation control. The system uses ZigBee technology to monitor the temperature and humidity of the environment. This article focuses on the hardware design for the collection and coordination of temperature and humidity data. Then, we will use ZigBee technology to develop and implement a star structure topology network with functions such as automatic network, environmental information collection, wireless data transmission, real-time LCD display, and serial data upload. Finally, the demand for network technology is measured based on forging and engraving tests. In addition, based on the rapid development of integrated sensors and wireless sensor technology, a high-precision, networked, on-site, and intelligent wireless temperature, and humidity measurement program was designed.

Data Availability

The data used to support the findings of this study are available from the corresponding author upon request.

Conflicts of Interest

The authors declare that they have no conflicts of interest.

References

[1] B. Aneja, S. Singh, U. Chandna, and V. Maheshwari, "Review of temperature measurement and control," *Ijarse Com*, vol. 3, no. 1, pp. 33–40, 2014.

[2] L. Yu, W. Wang, X. Zhang, and W. Zheng, *A Review on Leaf Temperature Sensor: Measurement Methods and Application. Computer and Computing Technologies in Agriculture IX*, Springer International Publishing, New York, NY, USA, 2015.

[3] L. L. Josephson, W. J. Galush, and E. M. Furst, "Parallel temperature-dependent microrheological measurements in a microfluidic chip," *Biomicrofluidics*, vol. 10, no. 4, Article ID 043503, 2016.

[4] G. Bonciolini, A. Demello, D. Vigolo, and E. Sciubba, "Microfluidic in-chip temperature control via the heat of mixing release," in *Proceedings of the ECOS 2016, International Conference on Efficiency, Cost, Optimisation, Simulation and Environmental Impact of Energy Systems*, Portorož, Slovenia, June 2016.

[5] X. Y. Chen, T. Y. Li, S. Zhang et al., "Research on optimizing parameters of thermal bonding technique for pmma microfluidic chip," *International Polymer Processing*, vol. 32, no. 3, pp. 394–398, 2017.

[6] L. Wang, Y. Yan, and K. Reda, "Comparison of single and double electrostatic sensors for rotational speed measurement," *Sensors and Actuators A: Physical*, vol. 266, pp. 46–55, 2017.

[7] D. M. Wan, K. Yang, Y. Y. Zhang, and K. N. Leung, "Design of temperature measurement system based on negative temperature coefficient," *China Medical Devices*, vol. 3, no. 11, pp. 98–103, 2017.

[8] C. Giebeler, D. Adelerhof, A. Kuiper, J. B. A. van Zon, D. Oelgeschläger, and G. Schulz, "Robust GMR sensors for angle detection and rotation speed sensing," *Sensors and Actuators A: Physical*, vol. 91, no. 1-2, pp. 16–20, 2001.

[9] L. Wang, Y. Yan, Y. Hu, and X. Qian, "Rotational speed measurement through electrostatic sensing and correlation signal processing," *IEEE Transactions on Instrumentation and Measurement*, vol. 63, no. 5, pp. 1190–1199, 2014.

[10] C. Li, Q. Tan, P. Jia et al., "Review of research status and development trends of wireless passive LC resonant sensors for harsh environments," *Sensors*, vol. 15, no. 6, pp. 13097–13109, 2015.

[11] B. Wang, M.-K. Law, J. Yi, C.-Y. Tsui, and A. Bermak, "A -12.3 DBm UHF passive RFID sense tag for grid thermal monitoring," *IEEE Transactions on Industrial Electronics*, vol. 66, no. 11, pp. 8811–8820, 2019.

[12] C. Li, Q. Tan, C. Xue, W. Zhang, Y. Li, and J. Xiong, "A high-performance LC wireless passive pressure sensor fabricated using low-temperature co-fired ceramic (LTCC) technology," *Sensors*, vol. 14, no. 12, pp. 23337–23347, 2014.

[13] C. Deng, W. Hu, S. X. Diao, F. Lin, and D. Qian, "Measurement error analysis and calibration technique of NTC-based body temperature sensor," *Chinese Journal of Medical Instrumentation*, vol. 39, no. 6, pp. 395–399, 2015.

[14] A. Farouk, A. Alahmadi, S. Ghose, and A. Mashatan, "Blockchain platform for industrial healthcare: vision and future opportunities," *Computer Communications*, vol. 154, pp. 223–235, 2020.

[15] P. Zhang, F. Wang, S. Yang, G. Wang, M. Yu, and X. Feng, "Flexible in-plane micro-supercapacitors: progresses and challenges in fabrication and applications," *Energy Storage Materials*, vol. 28, pp. 160–187, 2020.

[16] Y. T. Wu and Z. J. Pan, "The research status and development tendency of flexible wearable electronic sensors," *Modern Silk Science & Technology*, vol. 34, no. 5, pp. 22–25, 2019.

[17] M. D. Dankoco, G. Y. Tesfay, E. Benevent, and M. Bendahan, "Temperature sensor realized by inkjet printing process on flexible substrate," *Materials Science and Engineering: B*, vol. 205, no. 3, pp. 1–5, 2016.

[18] K. S. Karimov, F. A. Khalid, and T. M. S. Chani, "Carbon nanotubes based flexible temperature sensors," *Optoelectronics and Advanced Materials*, vol. 6, no. 1-2, pp. 194–196, 2012.

[19] S. Heidari, M. M. Abutalib, M. Alkhambashi, A. Farouk, and M. Naseri, "A new general model for quantum image histogram (QIH)," *Quantum Information Processing*, vol. 18, no. 6, pp. 175–220, 2019.

[20] K. Bennett and O. Mangasarian, "Combining support vector and mathematical programming methods for induction," *Advances in Kernel Methods—SV Learning*, vol. 1, pp. 307–326, 1999.

[21] C. Domeniconi and D. Gunopulos, "Incremental support vector machine construction," in *Proceedings of the IEEE International Conference on Data Mining (ICDM'01)*, pp. 589–592, San Jose, CA, USA, December 2001.

[22] J. Zhang, Z. Li, and J. Yang, "A divisional incremental training algorithm of support vector machine," in *Proceedings of the IEEE International Conference on Mechatronics and Automation (ICMA'05)*, pp. 853–856, Niagara Falls, ON, Canada, August 2005.